# Built-in-Self Test of Transmitter I/Q Mismatch and Nonlinearities Using Self-Mixing Envelope Detector

by

Srinath Byregowda

A Thesis Presented in Partial Fulfillment
of the Requirements for the Degree
Master of Science

Approved July 2012 by the
Graduate Supervisory Committee:

Sule Ozev, Chair
Yu Cao
Hongbin Yu

ARIZONA STATE UNIVERSITY

August 2012

ABSTRACT

Built-in-Self-Test (BiST) for transmitters is a desirable choice since it eliminates the reliance on expensive instrumentation to do RF signal analysis. Existing on-chip resources, such as power or envelope detectors, or small additional circuitry can be used for BiST purposes. However, due to limited bandwidth, measurement of complex specifications, such as IQ imbalance, is challenging. In this work, a BiST technique to compute transmitter IQ imbalances using measurements out of a self-mixing envelope detector is proposed. Both the linear and non linear parameters of the RF transmitter path are extracted successfully. We first derive an analytical expression for the output signal. Using this expression, we devise test signals to isolate the effects of gain and phase imbalance, DC offsets, time skews and system nonlinearity from other parameters of the system. Once isolated, these parameters are calculated easily with a few mathematical operations. Simulations and hardware measurements show that the technique can provide accurate characterization of IQ imbalances. One of the glaring advantages of this method is that, the impairments are extracted from analyzing the response at baseband frequency and thereby eliminating the need of high frequency ATE (Automated Test Equipment).

DEDICATION

Dedicated to my family and friends.

ACKNOWLEDGMENTS

I would like to acknowledge the enthusiastic supervision of Dr. Sule Ozev for her guidance, encouragement and more importantly providing me an opportunity to work on this novel idea. I would like to extend my sincere gratitude for guiding me through the process with a lot of patience

I also thank my committee members, Dr. Yu Cao and Dr.Honbin Yu, for their time and effort to help me fulfill the degree requirements. I am grateful to the RF Testlabs at the Arizona State University for all the support provided through out. In particular, I would like to thank Afsaneh Nassery and Ender Yilmaz who often made more efforts to help me find solutions to my hurdles while they had plenty to cross themselves. I would like to thank my old colleagues Yogan Senthilkumar, Kaliraj Gurusamy and other members of the RF test team at Tessolve Services Pvt. Ltd. for their timely guidance.

I am grateful to all my friends at Arizona State University for making my stay in Tempe, Arizona particularly enjoyable. I would like to thank my friend Mayur Agarwal for all the help during my transition to the new place and throughout my stay here. I would like to thank all the pretty girls who did not come out to coffee with me for saving the precious time that I spent in the lab and the ones who did come out for coffee for kind encouragement and motivation.

Finally, I would like thank my parents, brother, uncles, aunts, nieces and nephew who have been the support system and an inspiration throughout.

TABLE OF CONTENTS

Page

LIST OF TABLES ..... vi

LIST OF FIGURES ..... vii

CHAPTER

1 INTRODUCTION ..... 1

2 PRIOR WORK ..... 5

3 ARCHITECTURE AND MODELLING ..... 9

3.1 Quadrature Transmitter Architecture ..... 9

3.2 Modeling Of The Transmitter ..... 10

3.3 BIST Architecture - Envelope Detector ..... 12

4 EXTRACTION OF IMPAIRMENTS ..... 15

4.1 Linear Parameters ..... 15

4.2 Linear Parameter Extraction ..... 18

4.3 Computation Of Time Skews ..... 21

4.4 De-Embedding Gain Fluctuations ..... 21

4.5 Nonlinear Parameter Extraction ..... 22

5 EXPERIMENTAL RESULTS ..... 28

5.1 Simulation Results ..... 28

5.2 Hardware Measurement Results ..... 34

6 ADVANTAGES AND LIMITATIONS ..... 41

6.1 Advantages ..... 41

CHAPTER Page

6.2 Limitations ..... 41

7 CONCLUSION ..... 43

REFERENCES ..... 44

LIST OF TABLES

Table Page

1. Parameter Definition ..... 12

2. Summary of simulation results ..... 33

3. Hardware results of I/Q impairments extraction ..... 37

4. Hardware results of IIP3 extraction ..... 39

LIST OF FIGURES


Figure Page

1. I/Q modulation transmitter ..... 9
2. Proposed transmitter model with impairments and BiST circuitry ..... 11
3. BiST Circuitry ..... 13
4. Output Spectrum at the end of BiST circuitry ..... 17
5. Gain mismatch extraction error ..... 29
6. Phase mismatch extraction error ..... 29
7. DC offset extraction error on the I arm ..... 30
8. DC offset extraction error on the Q arm ..... 30
9. Differential delay extraction error ..... 31
10. Path gain extraction error ..... 31
11. IIP3 extraction error ..... 32
12. IIP2 extraction error ..... 33
13. Hardware measurement block diagram ..... 35
14. Hardware measurement setup ..... 35
15. Hardware measurement time domain output ..... 36
16. Hardware measurement spectrum output ..... 37
17. Test setup to measure IIP3 ..... 38

Chapter 1

# INTRODUCTION

With 6.2 billion mobile devices with network subscriptions today, that is expected to grow to 9 billion by 2017 [1], the market for RF devices is large and growing at a fast pace. Market share in the semiconductor consumer market is highly competitive. It is primarily driven by the cost and performance of the device. Continuous CMOS scaling and including more on chip structures to form a system-on-chip (SoC) are direct affects of performance scaling. However, both SoC implementation and shrinking of devices add to stringent specification requirement. Testing these stringent specifications needs expensive test equipment which would add to the cost of the device.

Test cost comprises a large share of the overall product cost for RF devices. Test cost is primarily driven by two factors, test time and test equipment cost. Efforts are consistently made to reduce test time as well as to provide test solutions on cheaper equipments.

Some of the typical tests performed on RF devices are Gain, Sensitivity, Noise figure, IIP3, P1dB, I/Q imbalances. Gain and sensitivity are a measure of the strength of the signal. Noise figure is

a measure of the noise added by the device. IIP3 and P1dB are a measure of the nonlinearities introduced by the device. These parameters determine linear region of the device. I/Q imbalances determine the mismatches in I (In Phase) and Q (Quadrature) paths. These mismatches if determined can be compensated during reception. All these parameters of the device have to be determined before releasing the device to the market. All these parameters have a direct relation with respect to the proper transmission and reception of the signal.

Expensive RF testers are required to perform these tests. Thus, considerable research effort needs to focus on reducing the reliance on these expensive RF testers. One of the approaches to achieve this goal is built-in-self-test (BiST). BiST circuitry can be designed using existing design components or may require additional circuitry. Additional circuitry results in increase in silicon cost. However, if simple circuits or existing resources can be used for BiST, this cost can be minimized.

Generally, BiST strategies for RF devices rely on down converting the signal from RF frequency to baseband frequencies. Several techniques

have been proposed to enable the RF to low frequency conversion [2]-[8]. Peak or power detectors are simple in terms of implementation [6]-[8] and introduce very little overhead. Using these kinds of detectors it is possible to measure the amplitude (or power) of the signal based on sine-wave approximation. Thus, parameters, such as 1 dB compression point, gain and third order input intercept can be measured.

While the characterization of the gain, noise figure, and IIP3 has been the target of almost all prior BiST work using sensors, other important parameters of transceivers such as IQ imbalances, have not been addressed. IQ imbalances, namely IQ gain and phase mismatch, DC offsets, time skews and non linearity (IIP2 and IIP3) are detrimental to the transceiver operation and thus need to be characterized. Moreover, these parameters are amenable to digital compensation [9]-[11]. Thus, in-field measurement and monitoring of such parameters are useful in the context of circuit adaptation.

In this work, we aim at characterizing the IQ imbalance parameters of transmitters using one self-mixing envelope detector at the end of transmitter chain. We first derive the output response of the complete model including the detector. Using this model, we devise specialized

test signals so that the effect of each impairment parameter can be decoupled. The signals are applied as digital patterns at the input of the transmitters. We only use the amplitude information to determine target parameters. Amplitudes of signal components can be easily, obtained using FFT at the desired frequency locations. Using our technique, the imbalance parameters can be computed with less than 1msec test time. In order to make these amplitude measurements, we use FFT on the low-frequency digitized signal. Digitization and signal processing can be done using already existing components in the system as most SOC's contain several house-keeping ADCs and processing units.

Chapter 2

# PRIOR WORK

Authors in [12] describe the test cost, time and equipment limitations associated with the test of various blocks of the SoC, such as digital circuits, mixed signal circuits, and memory. Test cost becomes a significant contributor to the production cost. Efforts to reduce the manufacturing cost include reducing ATE capital and operational cost as well as increasing throughput per ATE. BiST based solutions address both of these factors. It helps reduction of test time as it reduces the switching time of ATE instruments and measurement of complex circuitry using low cost testing solutions.

In most Built-in-Self-Test (BiST) techniques, a small piece of circuit is added to the design in order to convert the system response to a simpler form with lower frequency that makes on-chip analysis feasible [13] – [18]. This RF to low frequency conversion can be enabled using peak, power, or envelope detectors. Such BiST techniques have been proposed to characterize RF blocks, such as low noise amplifiers (LNAs), or power amplifiers (PAs), or the entire transmitter chain [6],[8], [13] – [15]. In [13], a BiST technique for LNA is presented. The BiST circuit detects amplitude alterations at the outputs of the

differential LNA, due to parametric or catastrophic faults, and provides a single digital Pass/Fail indication signal. An LNA BiST technique is presented in [14]. Input matching, gain, and output matching as well as the linearity of the CUT are measured. For input matching measurements, three sequential sinusoidal signals are used as input and the fluctuation in the LNA current is sensed using an envelope detector.

A loop-back based BiST technique for local oscillator, phase noise, RF front-end and baseband blocks of a transceiver are presented in [15]. A switch is used in the loop-back path as a frequency translator to generate two harmonics of the signal, which are used for magnitude characterization of RF section using several RF detectors. In [17], a loop-back BiST spectral signature analysis technique is proposed. OFDM signal is chosen as the spectral test signature. In [3], [15], on-chip sensor responses are used to predict the performance parameters of the RF blocks and system specifications (IIP3, gain, and NF) using a non-linear regression model. In [3], the authors also present an optimized algorithm for sensor placement.

Envelope detectors are widely used in BiST techniques for testing various RF blocks since the envelope of the high frequency signal preserves important information [6], [8], [19] – [20]. In [8], the envelope of the circuit response to a two tone test stimuli is captured and its wavelet coefficients are used to predict the gain, NF and P1dB of the circuit using a Multivariate Adaptive Regression Splines (MARS) model. Another method using the envelope of the circuit response with respect to a 2-tone input is presented in [6]. Spectral information is used to define a digital signature. As the signature range is known for acceptable DUTs, a go/no-go test output signal is generated. Most of this prior work on Built-in-Self-Test for RF circuits focuses on the characterization of noise figure, gain, and nonlinearity of the devices. However IQ imbalances, namely IQ gain and phase mismatch, DC offsets, and time skews are detrimental to the transceiver operation and thus need to be characterized. Moreover, these parameters are amenable to digital compensation [9], [21] – [22]. Thus, in-field measurement and monitoring of such parameters are useful in the context of circuit adaptation. In [10] - [11], the authors present a technique to extract a more complete set of transceiver impairment parameters using the loop-back configuration and non-linear solvers. However, due to computational complexity, these

approaches are more suitable for tester implementation. In this work, we aim at characterizing the IQ imbalance parameters of the transmitters using a self-mixing envelope detector.

Chapter 3

# ARCHITECTURE AND MODELLING

## 3.1 QUADRATURE TRANSMITTER ARCHITECTURE

In an I/Q modulation scheme, I and Q signals are modulated using sine and cosine signal that are orthogonal to each other. Thus, two uncorrelated bit streams can be modulated at the same time without increasing the bandwidth. However, orthogonal behavior of these signals is essential for the proper operation of the transmitter.

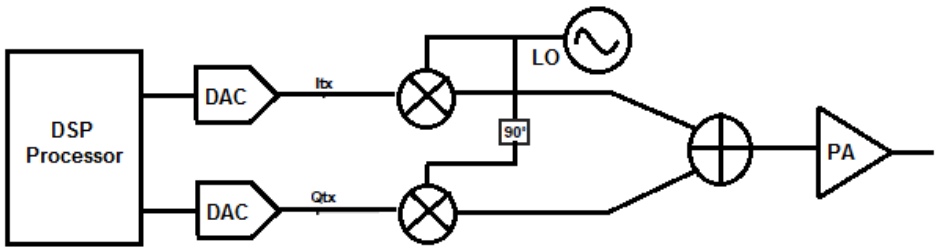


Fig. 1: I/Q Modulation Transmitter

A simple I/Q modulating transmitter is depicted in Fig.1. A bit stream is generally transmitted using this transmitter. The bit stream is generated by the DSP processor. The digital bit stream needs to be converted to analog signal for transmission. These signals pass through a mixer in the respective I and Q path. The mixer up converts the baseband signal to the desired RF frequency. The other signal for

the mixer is generated from the Local Oscillator. The frequency of the LO is selected based on the transmission frequency. The phase difference between the two LO signals to I and Q path should be $90^o$ This phase difference is obtained by passing the signal through a $90^o$ phase shifter. The high frequency output signals from the I and Q mixers are added to form the desired RF signal. This RF signal is passed through a Power Amplifier (PA) to enable long distance transmission. This analog signal is captured using a quadrature receiver at the other end.

## 3.2: MODELING OF THE TRANSMITTER

Orthogonality between I and Q channels preserves the information in limited bandwidth. However, this also makes the transmitter sensitive to mismatches between I and Q arms. Orthogonality requires that the two arms have a perfect match in gain, and exactly 90 degrees phase shift. Any deviation from this ideal point will cause leakage from I to Q and vice versa. This leakage acts as noise and degrades the transmission quality. Similarly, DC offsets generate carrier leakage and can be detrimental for the proper operation of transmission and reception. It can also result in unnecessary saturation in the path. Thus they need to be characterized for the transmitter. In addition to

these parameters, the non-linearity of the power amplifier needs to be characterized since it both degrades modulation quality and results in spectral growth into other bands/channels.

In order to model, analyze, and compute these impairments, the transmitter shown in the Fig.1 is now revised to a new model as shown in Fig.2 with all these impairments. Fig. 2 shows the transmitter system block diagram including the proposed BiST circuit that will be explained in next section. In this model, we include gain and phase imbalances between I and Q arms. DC offsets and time skews are also included in the model. Non-linearity of the transmitter path is modeled as second and third order polynomial gain function covering for the power amplifier. Eqn. (1) shows the RF signal relation at the output of the transmitter in linear mode in terms of input signals at I and Q arms including all of these system-level parameters given in Table I.

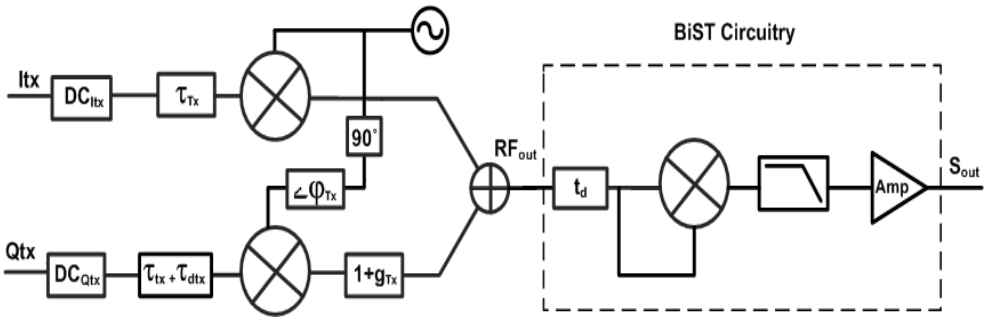


Fig 2: Proposed transmitter model with impairments and BiST circuitry

$$RF_{out}(t) = G(I(t-\tau_{tx}) + DC_{Itx})\cos(\omega_c t) + G(Q(t-\tau_{dtx}-\tau_{tx}) + DC_{Qtx})(1+g_{tx})\sin(\omega_c t_d + \varphi_{tx})) \quad (1)$$

| Parameter | Symbol Representation |
|---|---|
| Gain Mismatch | $g_{tx}$ |
| Phase mismatch | $\varphi_{tx}$ |
| TX DC Offsets | $DC_{Itx}$, $DC_{Qtx}$ |
| Baseband Time Skew | $\tau_{dtx}$ |
| Baseband Delay | $\tau_{tx}$ |
| Self Mixing Delay | $t_d$ |
| Path Gain | G, G2, G3 |
| Self Mixing Attenuation | K |

TABLE I ：Parameter definition

All the impairments are modeled in the Q arm with respect to I arm. However, it can be modeled vice versa or distributed equally among both of them. Each model can be solved with similar approach and the results obtained would be identical.

3.3: BIST ARCHITECTURE - ENVELOPE DETECTOR.

Generally in RF BiST techniques, the high frequency circuit response is converted into a low frequency form which is easier to analyze on-chip. The conversion needs to carry all the information pertaining to the desired parameters. For this purpose, a self-mixing envelope detector is used as shown in Fig. 3. This detector basically multiplies the transmitter output with itself, generating a low-frequency component, and a high frequency component. The high frequency component is filtered by the Low Pass Filter. DC and Low frequency component is now available for spectral analysis. The BiST mixer needs to be of special 4-quadrant architecture and if it cannot be driven with a low power from the LO port, an amplifier may be necessary in this path. Similar detector architectures have been included in commercial devices to monitor and adjust the transmitter output power. Thus, such existing detectors can be used for BiST purposes. The output signal from the detector is digitized and analyzed. A generic on-chip ADC and processor can be used for this purpose.

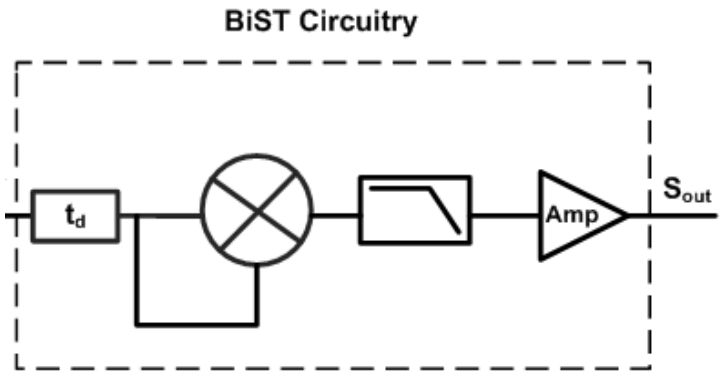

Fig 3: BiST circuitry

The above transmitter model along with the BiST circuitry as shown in Fig. 2 is modeled by building each block with its respective mathematical function in Mathematica. The behavior of the model is analyzed by observing the output equation of the model.

Chapter 4

# EXTRACTION OF IMPAIRMENTS

## 4.1: LINEAR PARAMETERS

Parameters of the device that change linearly are classified as linear parameters. And those that change nonlinearly are called nonlinear parameters. Gain, Noise figure, I/Q imbalances, DC Offsets are linear parameters and parameters such as P1dB and IIP3 are nonlinear. Most devices behave linearly in the small signal power. Hence, while extracting linear parameters all the blocks in the model are modeled in small signal power. The whole system is considered to be linear while operating in linear power. It has to be ensured that the input power is not high enough to excite the system in to nonlinearities while extracting linear parameters.

To measure a nonlinear parameter, the system has to be excited in the nonlinear mode. The input power should be high enough to drive the system in the nonlinear mode, if not the extracted measurements will not be accurate. It can be seen later that output of the system changes between the linear and nonlinear mode.

Using the behavior of the blocks in Fig.2, the output of the detector can be expressed in terms of the transmitter inputs I(t) and Q(t) as in Eqn. (2):

$$\begin{aligned} S_{out}(t) = & \frac{1}{2}\left(\frac{G}{K}\right)^2 (DC_{Itx}{}^2 + (1+g_{tx})^2 DC_{Qtx}{}^2) + \left(\frac{G}{K}\right)^2 (1+g_{tx}) DC_{Itx} DC_{Qtx} \sin(\varphi_{tx}) \\ & + \left(\frac{G}{K}\right)^2 (DC_{Itx} + (1+g_{tx}) \sin(\varphi_{tx}) DC_{Qtx}) I(t-\tau_{tx}-t_d) \\ & + \left(\frac{G}{K}\right)^2 I^2(t-\tau_{tx}-t_d) + \left(\frac{G}{K}\right)^2 (1+g_{tx})(DC_{Itx} \sin(\varphi_{tx}) + (1+g_{tx}) DC_{Qtx}) Q(t-\tau_{tx}-\tau_{dtx}-t_d) \\ & + \frac{1}{2}\left(\frac{G}{K}\right)^2 (1+g_{tx})^2 Q^2(t-\tau_{tx}-\tau_{dtx}-t_d) + \left(\frac{G}{K}\right)^2 (1+g_{tx}) \sin(\varphi_{tx}) I(t-\tau_{tx}-t_d) Q(t-\tau_{tx}-\tau_{dtx}-t_d) \end{aligned} \quad (2)$$

Eqn. (2) shows that while the effect of the impairments can be observed at the output, these effects are convoluted in the overall signal and separation of these parameters is not straightforward. Thus, we need to devise a clever test signal that will help us separate out each of these terms. First, we observe from Eqn. (2) that using complex modulated signals is not a desirable choice since the baseband signals and their delayed components cannot be easily expressed in closed form mathematical equations. Another alternative is to use sinusoidal signals. Here, one has to pay particular attention to what frequency signals are included in the baseband terms. For instance, if both arms are excited by a signal at the same frequency (i.e., I(t) = $\cos(\omega_1 t)$ and Q(t) = $\sin(\omega_1 t)$), then all the information will be contained in DC and (2 $\omega_1 t$). Separating variables is not straightforward.

However, if the frequencies of the two signals are distinct, (i.e., I(t) = cos ($\omega_1 t$) and Q(t) = cos ($\omega_2 t$)), then the information will be separated out to DC, $\omega_1$, $\omega_2$, 2 $\omega_1$, 2 $\omega_2$, ($\omega_1$ + $\omega_2$) and ($\omega_1$ - $\omega_2$) frequencies. This separation generates a larger number of simpler equations to enable analytical computation. Based on these input signals, Fig. 4 shows an example of the BiST output spectrum.

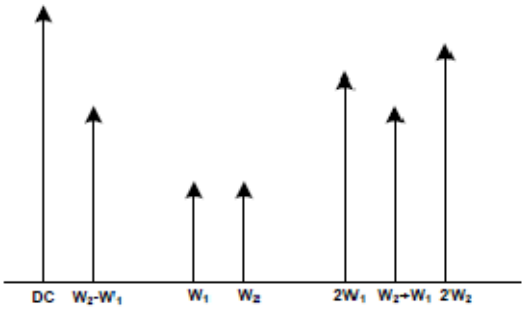


Fig. 4: Output Spectrum at the end of BiST circuitry.

Note that the input frequency locations have to be chosen in a way that none of the intermodulation products overlap with each other. The frequency domain information can be used to solve for the desired impairments if there are enough independent equations. Substituting the designed test signal into Eqn. (2) and simplifying the result shows that we can use the amplitude of the frequency terms in order to separate the effect of these nonidealities and solve for them mathematically. Eqn. (3) shows the amplitude expression for each of the frequency locations.

$$A_{DC} = \frac{1}{2}\left(\frac{G}{K}\right)^2\left(\frac{1}{2}+\frac{1}{2}(1+g_{tx})^2 + DC_{Itx}{}^2 + (1+g_{tx})^2 DC_{Qtx}{}^2\right) + \left(\frac{G}{K}\right)^2 (1+g_{tx}) DC_{Itx} DC_{Qtx} \sin(\varphi_{tx})$$

$$A_{w1} = \left(\frac{G}{K}\right)^2 DC_{Itx} + (1+g_{tx}) DC_{Qtx} \sin(\varphi_{tx})$$

$$A_{w2} = \left(\frac{G}{K}\right)^2 (1+g_{tx}) DC_{Itx} \sin(\varphi_{tx}) + \left(\frac{G}{K}\right)^2 (1+g_{tx})^2 DC_{Qtx}$$

$$A_{2w1} = \frac{1}{4}\left(\frac{G}{K}\right)^2$$

$$A_{2w2} = \frac{1}{4}\left(\frac{G}{K}\right)^2 (1+g_{tx})^2$$

$$A_{w1+w2} = \frac{1}{2}\left(\frac{G}{K}\right)^2 (1+g_{tx}) \sin(\varphi_{tx})$$

$$A_{w1-w2} = \frac{1}{2}\left(\frac{G}{K}\right)^2 (1+g_{tx}) \sin(\varphi_{tx}) \qquad (3)$$

## 4.2: LINEAR PARAMETER EXTRACTION

To extract the linear impairments, it has to be ensured that the system is operated in low power (in the linear range). Since the amplifier is the main contributor for the nonlinearity, it is assumed that the complete system is linear provided the input to the amplifier is low. The behavior of the amplifier is modeled as Eqn. 4.

$$y(t) = x(t) * G \qquad (4)$$

With the two tone input signal as discussed in the previous section, we have 7 frequency locations to analyze, as in Eqn. (3). We also have 5 unknowns ($\left(\frac{G}{K}\right)$, $g_{tx}$, $\varphi_{tx}$, $DC_{Itx}$ and $DC_{Qtx}$). However, as Eqn. (3) indicates, expressions for the two frequencies (ω1 + ω2) and (ω1 - ω2) have the same amplitude, so they provide only one linearly independent equation. The DC term is unreliable even though it provides an additional equation. The DUT LO leakage can be mixed with itself and produce an undesired DC component that can alter the accuracy of the computation, or DC term may be corrupted by any DC offset that is generated by the detector, which is not included in the model. Thus, Eqn. (3) yields 5 usable linearly independent equations with 5 unknowns. We also observe that by taking a step-by-step approach, the unknowns can be analytically solved.

Computation of Gain, Phase mismatch and DC offsets.

Step 1: The path gain is extracted using the amplitude of the (2ω1) term as in Eqn. (5):

$$\left(\frac{G}{K}\right) = \sqrt{4 \times A_{2w1}} \qquad (5)$$

Note that the path gain includes the gain of the transmitter (G) as well as the gain of the detector (1/K). As a matter of fact, using a detector in the linear operation range, these two parameters cannot be separated

from one another. However, since the terms G and K always appear together, computing (G/ K) in the first step is adequate to compute the IQ imbalance parameters.

Step 2: The amplitude at the 2 ω2 frequency along with the already computed path gain are used to compute the gain mismatch as shown in Eqn. (6).

$$g_{tx} = \sqrt{\frac{A_{2w2}}{\frac{1}{4}\left(\frac{G}{K}\right)^2}} - 1 \qquad (6)$$

Step 3: Eqn. (3) shows that the remaining unknown in the amplitude of the terms at (ω1 + ω2) or (ω1 - ω2) frequencies is the phase mismatch. It can be computed using Eqn. (7).

$$\varphi_{tx} = \sin^{-1}\left(\frac{A_{w1-w2}}{\frac{1}{2}\left(\frac{G}{K}\right)^2 (1+g_{tx})}\right) \qquad (7)$$

Step 4: In order to solve for the DC offsets, we make use of information at the frequency locations ω1 and ω2. Eqn. (8) shows the mathematical expression for I and Q DC offset computation.

$$DC_{Itx} = \frac{A_{w1}(1+g_{tx}) - A_{w2}\sin(\varphi_{tx})}{\left(\frac{G}{K}\right)^2 (1+g_{tx})\cos^2(\varphi_{tx})}$$
$$DC_{Qtx} = \frac{A_{w2} - A_{w1}(1+g_{tx})\sin(\varphi_{tx})}{\left(\frac{G}{K}\right)^2 (1+g_{tx})^2\cos^2(\varphi_{tx})} \quad (8)$$

## 4.3: COMPUTATION OF TIME SKEWS

We have analyzed the frequency components of the envelope signal in terms of amplitude. The phases of these signals are a function of delays in the baseband path. If we measure these delays, the time skews can be calculated simply as the difference between the phases of the signal components at 2ω1 and 2ω2 frequencies as Eqn. (9):

$$\tau_{dtx} = \frac{\arg(2\omega 1)}{2\omega 1} - \frac{\arg(2\omega 2)}{2\omega 2} \quad (9)$$

Note that any delay that is added to the signal in test path, and not modeled will be added to both I and Q arms and thus will not alter $\tau_{dtx}$ computation.

## 4.4. DE-EMBEDDING GAIN FLUCTUATIONS

In some cases, the amplifiers used in the path either as a part of the circuit under test or as a part of the BiST circuit, may exhibit fluctuations in the gain. This is more of a problem for baseband operation where the test signals are spread through a large portion of

pass band as opposed to RF operation where several MHz separations are not significant. In order to prevent the gain fluctuations from corrupting the computation of the parameters of interest, it may be necessary to parameterize gain at multiple frequency locations. Note that in our technique, we have 5 frequency locations to characterize. A carefully crafted test signal is used to characterize the parameter G/K at the desired frequency locations before moving into the other steps of computation. Thus step 1 is repeated 4 times to obtain the G/K variable to be used in steps 2 through 4. Additional calibration of the BIST circuit may be necessary to suppress unwanted components if leakage becomes a dominant factor.

## 4.5: NONLINEAR PARAMETER EXTRACTION.

To extract the nonlinear impairments, it has to be ensured that the system is operated in nonlinear range. Since the amplifier is the main contributor for the nonlinearity, it's assumed that the complete system is nonlinear provided the input to the amplifier is high. The behavior of the amplifier is now modeled as in Eqn. 10

$$y(t) = x(t)*G + x(t)^2 * G2 + x(t)^3 * G3 \qquad (10)$$

If the nonlinear model is excited with the same stimuli as the one used for the linear model, the output response at the end of the BiST circuit will be as shown in Eqn. 11. As seen the output has more frequency terms at the baseband.

$$A_{2w1-4w2} = \frac{45G3^2Gq^4}{512K^2} - 2\left(\frac{15G3^2Gq^4\text{Cos}[2\phi tx]}{512K^2}\right)$$

$$A_{2w1-2w2} = \left(\frac{3G2^2Gq^2}{16K^2} + \frac{3G1G3Gq^2}{8K^2} + \frac{45G3^2Gq^2}{128K^2} + \frac{45G3^2Gq^4}{128K^2} + 2\left(-\frac{3G2^2Gq^2}{64K^2} - \frac{3G1G3Gq^2}{32K^2} - \frac{15G3^2Gq^2}{128K^2} - \frac{15G3^2Gq^4}{128K^2}\right)\text{Cos}[2\phi tx]\right)$$

$$A_{4w1-2w2} = \frac{45G3^2Gq^2}{512K^2} + \frac{2(15G3^2Gq^2\text{Cos}[2\phi tx]}{512K^2}$$

$$A_{2w1+2w2} = \frac{3G2^2Gq^2}{16K^2} + \frac{3G1G3Gq^2}{8K^2} + \frac{45G3^2Gq^2}{128K^2} + \frac{45G3^2Gq^4}{128K^2} + 2\left(-\frac{3G2^2Gq^2}{64K^2} - \frac{3G1G3Gq^2}{32K^2} - \frac{15G3^2Gq^2}{128K^2} - \frac{15G3^2Gq^4}{128K^2}\right)\text{Cos}[2\phi tx]$$

$$A_{4w1+2w2} = \frac{45G3^2Gq^2}{512K^2} - 2\left(\frac{15G3^2Gq^2\text{Cos}[2\phi tx]}{512K^2}\right)$$

$$A_{2w1+4w2} = \frac{45G3^2Gq^4}{512K^2} - 2\left(\frac{15G3^2Gq^4\text{Cos}[2\phi tx]}{512K^2}\right)$$

$$A_{2w1} = \left(\frac{G1^2}{4K^2} + \frac{3G2^2}{16K^2} + \frac{3G1G3}{8K^2} + \frac{75G3^2}{512K^2} + \frac{3G2^2Gq^2}{8K^2} + \frac{3G1G3Gq^2}{4K^2} + \frac{45G3^2Gq^2}{64K^2} + \frac{135G3^2Gq^4}{256K^2}\right) + 2\left(-\frac{3G2^2Gq^2}{32K^2} - \frac{3G1G3Gq^2}{16K^2} - \frac{15G3^2Gq^2}{64K^2} - \frac{45G3^2Gq^4}{256K^2}\right)\text{Cos}[2\phi tx]$$

$$A_{4w1} = \left(\frac{3G2^2}{64K^2} + \frac{3G1G3}{32K^2} + \frac{15G3^2}{256K^2} + \frac{45G3^2Gq^2}{256K^2} - 2\left(\frac{15G3^2Gq^2\text{Cos}[2\phi tx]}{256K^2}\right)\right)$$

$$A_{6w1} = \frac{5G3^2}{512K^2}$$

$$A_{2w2} = \left(\frac{G1^2Gq^2}{4K^2} + \frac{3G2^2Gq^2}{8K^2} + \frac{3G1G3Gq^2}{4K^2} + \frac{135G3^2Gq^2}{256K^2} + \frac{3G2^2Gq^4}{16K^2} + \frac{3G1G3Gq^4}{8K^2} + \frac{45G3^2Gq^4}{64K^2} + \frac{75G3^2Gq^6}{512K^2} + 2\left(-\frac{3G2^2Gq^2}{32K^2} - \frac{3G1G3Gq^2}{16K^2} - \frac{45G3^2Gq^2}{256K^2} - \frac{15G3^2Gq^4}{64K^2}\right)\text{Cos}[2\phi tx]\right)$$

$$A_{4w2} = \frac{3G2^2Gq^4}{64K^2} + \frac{3G1G3Gq^4}{32K^2} + \frac{45G3^2Gq^4}{256K^2} + \frac{15G3^2Gq^6}{256K^2} - 2\left(\frac{15G3^2Gq^4\text{Cos}[2\phi tx]}{256K^2}\right)$$

$$A_{6w2} = \frac{5G3^2Gq^6}{512K^2}$$

$$A_{w1-3w2} = -2\left(\frac{15G3^2Gq^3\text{Sin}[3\phi tx]}{512K^2}\right) + 2\left(\frac{3G2^2Gq^3}{32K^2} + \frac{3G1G3Gq^3}{16K^2} + \frac{135G3^2Gq^3}{512K^2} + \frac{75G3^2Gq^5}{512K^2}\right)\text{Sin}[\phi tx]$$

$$A_{3w1-3w2} = -2\left(\frac{5G3^2Gq^3\text{Sin}[3\phi tx]}{512K^2}\right) + 2\left(\frac{45G3^2Gq^3\text{Sin}[\phi tx]}{512K^2}\right)$$

$$A_{w1-w2} = -2\left(\frac{45G3^2Gq^3\text{Sin}[3\phi tx]}{512K^2}\right) + 2\left(\frac{G1^2Gq}{4K^2} + \frac{9G2^2Gq}{32K^2} + \frac{9G1G3Gq}{16K^2} + \frac{75G3^2Gq}{256K^2} + \frac{9G2^2Gq^3}{32K^2} + \frac{9G1G3Gq^3}{16K^2} + \frac{405G3^2Gq^3}{512K^2} + \frac{75G3^2Gq^5}{256K^2}\right)\text{Sin}[\phi tx]$$

$$A_{3w1-w2} = -2\left(\frac{15G3^2Gq^3\text{Sin}[3\phi tx]}{512K^2}\right) + 2\left(\frac{3G2^2Gq}{32K^2} + \frac{3G1G3Gq}{16K^2} + \frac{75G3^2Gq}{512K^2} + \frac{135G3^2Gq^3}{512K^2}\right)\text{Sin}[\phi tx]$$

$$A_{w1+w2} = -2\left(\frac{45G3^2Gq^3Sin[3\phi tx]}{512K^2}\right) + 2\left(\frac{G1^2Gq}{4K^2} + \frac{9G2^2Gq}{32K^2} + \frac{9G1G3Gq}{16K^2} + \frac{75G3^2Gq}{256K^2} + \frac{9G2^2Gq^3}{32K^2} + \frac{9G1G3Gq^3}{16K^2} + \frac{405G3^2Gq^3}{512K^2} + \frac{75G3^2Gq^5}{256K^2}\right)Sin[\phi tx]$$

$$A_{3w1+w2} = -2\left(\frac{15G3^2Gq^3Sin[3\phi tx]}{512K^2}\right) + 2\left(\frac{3G2^2Gq}{32K^2} + \frac{3G1G3Gq}{16K^2} + \frac{75G3^2Gq}{512K^2} + \frac{135G3^2Gq^3}{512K^2}\right)Sin[\phi tx]$$

$$A_{w1+3w2} = -2\left(\frac{15G3^2Gq^3Sin[3\phi tx]}{512K^2}\right) + 2\left(\frac{3G2^2Gq^3}{32K^2} + \frac{3G1G3Gq^3}{16K^2} + \frac{135G3^2Gq^3}{512K^2} + \frac{75G3^2Gq^5}{512K^2}\right)Sin[\phi tx]$$

$$A_{3w1+3w2} = -2\left(\frac{5G3^2Gq^3Sin[3\phi tx]}{512K^2}\right) + 2\left(\frac{45G3^2Gq^3Sin[\phi tx]}{512K^2}\right)$$

$$A_{w1-5w2} = 2\left(\frac{15G3^2Gq^5Sin[\phi tx]}{512K^2}\right)$$

$$A_{5w1-w2} = 2\left(\frac{15G3^2GqSin[\phi tx]}{512K^2}\right)$$

$$A_{5w1+w2} = 2\left(\frac{15G3^2GqSin[\phi tx]}{512K^2}\right)$$

$$A_{w1+5w2} = 2\left(\frac{15G3^2Gq^5Sin[\phi tx]}{512K^2}\right) \qquad (11)$$

However, not all the frequency terms provide us the equations necessary to solve the variables. For pure mathematical analysis, all the variables namely $\left(\frac{G}{K}\right)$, $g_{tx}$, $\varphi_{tx}$, $\left(\frac{G2}{K}\right)$ and $\left(\frac{G3}{K}\right)$ can be extracted by solving the response analytically. But to do so the amplitude at DC has to be considered. However, for practical cases the measurement of the amplitude at DC can have other factors such as leakage of the self

mixing mixer and is not a recommended practice to depend upon amplitude at DC.

Here we can take advantage of the fact that we have already extracted the G/K, phtx and gtx from the linear analysis. Also, extraction of these variables yield better results in the linear mode than in the nonlinear mode. This reduces the number of variables to be extracted to 2 namely G2/K and G3/K.

Computation of G2/K and G3/K:

$$\left(\frac{G3}{K}\right)=\sqrt{(512/5)\times A_{6w1}} \qquad (12)$$

In order to solve for $\left(\frac{G3}{K}\right)$, we make use of the information at 6ω1. Eqn. 12 shows mathematical expression to extract $\left(\frac{G3}{K}\right)$.

$$\left(\frac{G2}{K}\right)=\sqrt{\left(\begin{array}{l}((15/256)\times 2\times\left(\frac{G3}{K}\right)^2(1+g_{tx})^2\cos(2\varphi_{tx})+A_{4w1})-(3/32)\times\left(\frac{G3}{K}\right)\left(\frac{G}{K}\right)\\ -(45/256)\times\left(\frac{G3}{K}\right)^2(1+g_{tx})^2-(15/256)\times\left(\frac{G3}{K}\right)^2\end{array}\right)}\times(64/3) \qquad (13)$$

Once we have the $\left(\frac{G3}{K}\right)$ extracted, along with the I/Q imbalances extracted in the linear phase and amplitude information at 4ω1, $\left(\frac{G2}{K}\right)$

can be extracted. Eqn. 13 shows mathematical expression to extract $\left(\frac{G2}{K}\right)$.

Chapter 5

# EXPERIMENTAL RESULTS

## 5.1: SIMULATION RESULTS

A Matlab based model is implemented as in Fig. 2. The accuracy of the proposed test technique is confirmed using Monte Carlo simulations, where random samples are taken for each of the unknowns within a given window. The limits are chosen quite wide and a large number of simulations are conducted to validate the technique for both severe impairment and marginal impairment scenarios. For test signal frequencies, it is beneficial to use a high separation between the signal tones. As a result, we need to ensure that all desired signal components fall into the bandwidth. We need to choose two frequencies which are as far apart as possible, but also satisfy bandwidth constraint. Thus, we have chosen 4MHz and 5MHz as test signal frequencies while LO frequency is 2.4GHz.

The below figures show the error of extraction for I/Q imbalances in the linear mode. It is seen that the errors are within acceptable range.

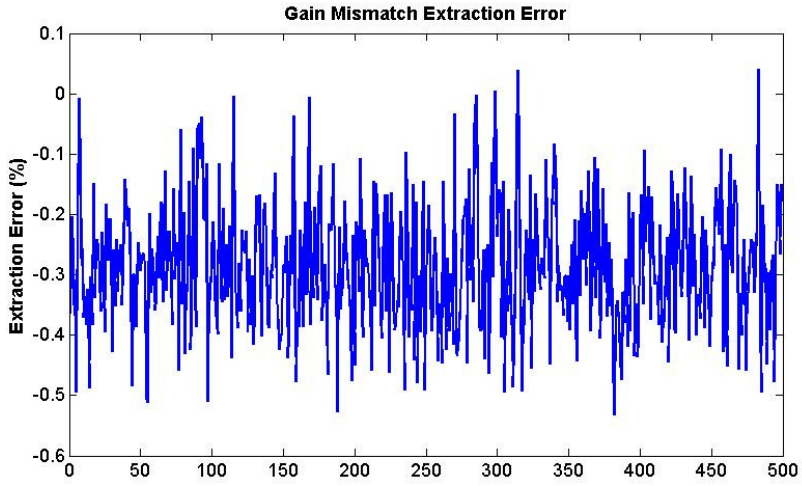


Fig. 5: Gain mismatch extraction error

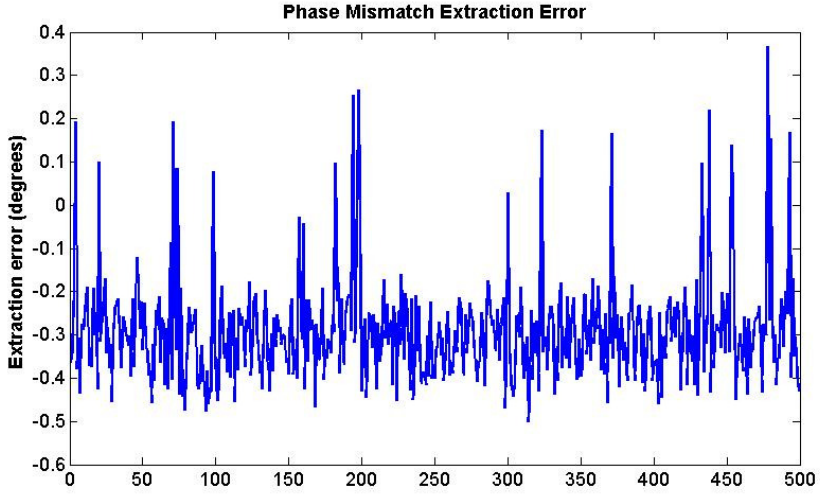


Fig. 6: Phase mismatch extraction error

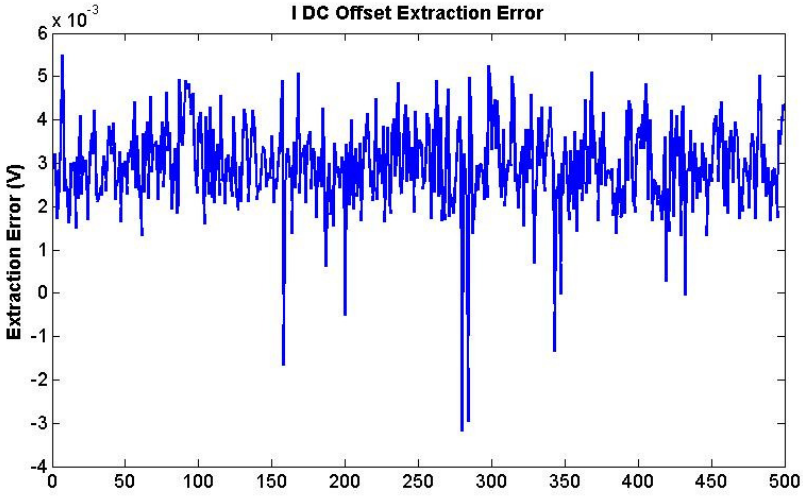


Fig. 7: DC offset extraction error on the I arm

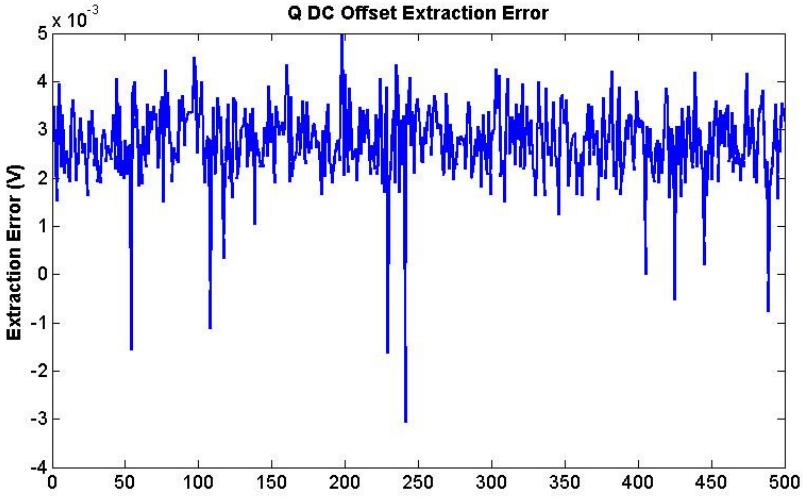


Fig. 8: DC offset extraction error on the Q arm

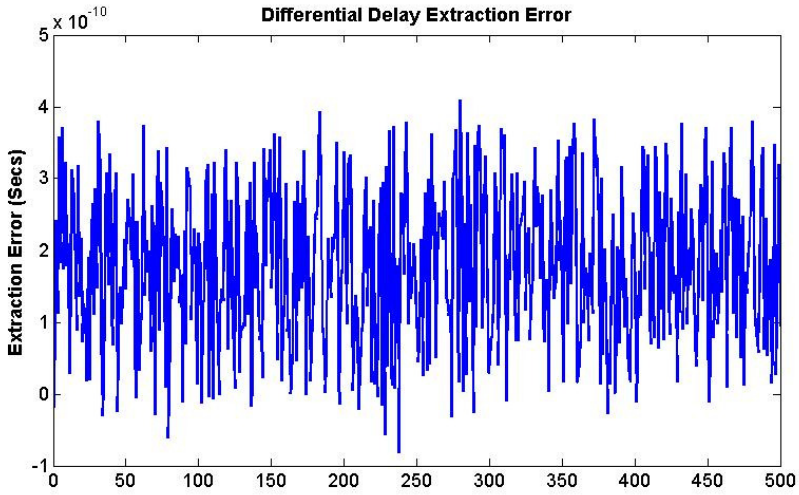


Fig. 9: Differential delay extraction error

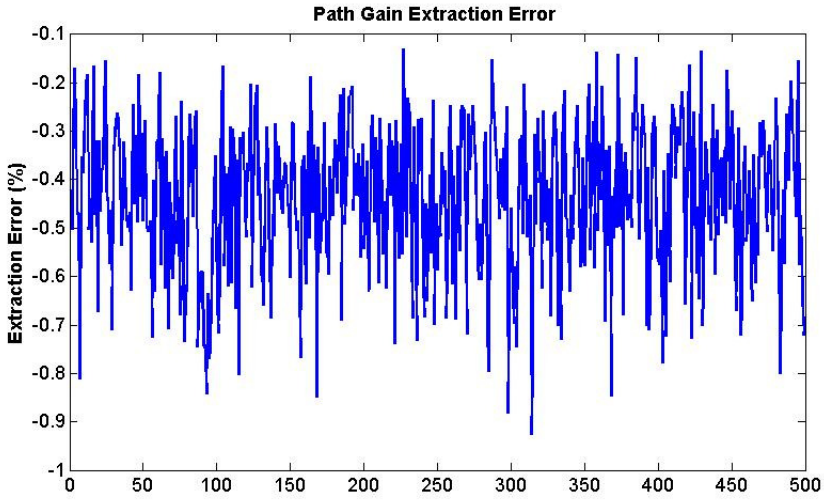


Fig. 10: Path gain extraction error

G3 affects the linearity of the system. However, the extraction of G3/K by itself will not give us much information because of the presence of (1/K). The amount of nonlinearity of the system is characterized by IIP3 of the system. It is as given by Eqn. 14

$$IIP3 = 20\log\left(\sqrt{\left(\frac{4}{3}\right)\left(\frac{G}{G3}\right)}\right) \qquad (14)$$

By substituting $\left(\frac{G}{K}\right)$ and $\left(\frac{G3}{K}\right)$ in Eqn. 14 (1/K) term in both $\left(\frac{G}{K}\right)$ and $\left(\frac{G3}{K}\right)$ gets cancelled and IIP3 can still be extracted. Fig. 11 shows the 500 run Montecarlo simulation result of the extraction error of IIP3.

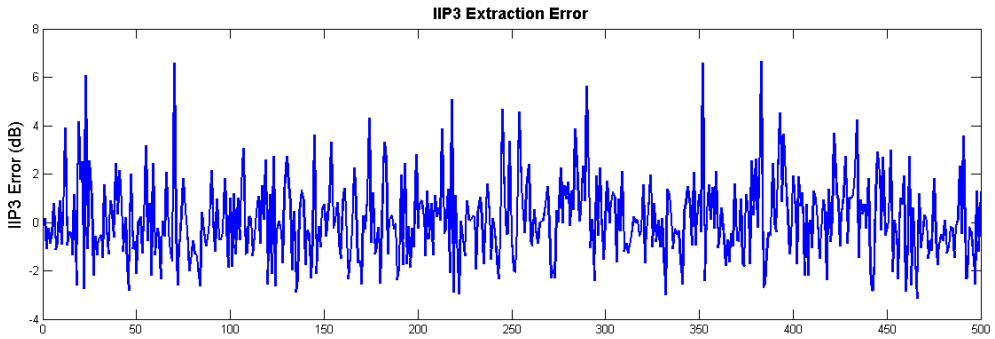


Fig. 11: IIP3 extraction error

Similar to G3, G2 also affects the linearity of the system but the affect is not as critical as that of G3. Extraction of $\left(\frac{G2}{K}\right)$ does not provide us with any information of the system. However, IIP2 of the system is a good measure of linearity of the system. It can be calculated by substituting $\left(\frac{G}{K}\right)$ and $\left(\frac{G2}{K}\right)$ in place of G and G2 respectively in eqn. 15.

$$IIP2 = 20\log\left(\left(\frac{G}{G2}\right)\right) \qquad (15)$$

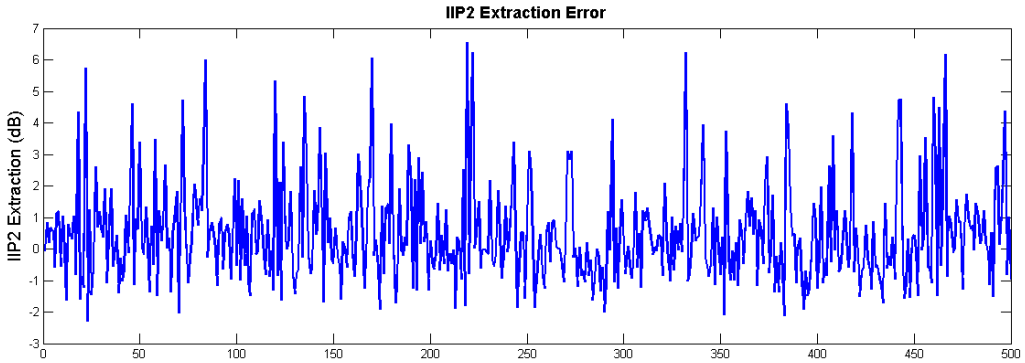

Fig. 12: IIP2 extraction error

| Parameter | RMS Error | Injection Limit |
|---|---|---|
| $\left(\frac{G}{K}\right)$ | 0.47% | [0.4, 2.5] |
| $\varphi_{tx}$ | 0.32° | [0°,5°] |
| $g_{tx}$ | 0.32% | [-20%, 20%] |
| $DC_{Itx}$ | 3mV | [0mV,50mV] |
| $DC_{Qtx}$ | 2.8mV | [0mV,50mV] |
| $\tau_{dtx}$ | 0.2ns | [0ns,5ns] |
| IIP2 | 1.62dB | [4.9dB, 7.95dB] |
| IIP3 | 1.66dB | [11.2dB, 14.25dB] |

TABLE II: Summary of simulation results

Fig. 12 shows the 500 run Montecarlo simulation result of the extraction error of IIP2. In some of the cases in Fig.11 and Fig.12, the error in extraction is high. The reason for this is ripple in the filter.

And any small change in the amplitude extraction of G3 and G2 can result in large errors in IIP3 and IIP2 extraction. By reducing the ripple in the designed filter, the error can be reduced.

Monte Carlo simulation bounds as well as RMS errors for 500 instances are shown in Table II. Table II indicates that RMS errors are negligible for the device operation. Low complexity of the proposed measurement as well as the accuracy of the method makes it a suitable candidate for on chip implementation

## 5.2: HARDWARE MEASUREMENT RESULTS

In order to make sure that unmodeled effects do not invalidate the proposed approach, we have implemented the BiST circuitry in hardware and performed the experiment on a transmitter which is a Vector Signal Generator (VSG). The hardware measurement block diagram is shown in Fig. 13. A vector signal generator (Rohde & Schwarz SMBV100A) is used for the transmitter path. The test signal is fed to I/Q modulator blocks. I/Q mismatch can be injected in VSG path. Off-the-shelf components from Mini-Circuits are used to build the BiST circuitry: mixer (ZFM - 15 - $S^+$) , power splitter/combiner(ZFSC – 2 – 4 - $S^+$) , low pass filter (SBLP – 117$^+$). A picture of the set up is shown in Fig. 14. Similar to the simulations, in

the measurements, the input frequencies are chosen as 5MHz for I and 4MHz for Q channel.

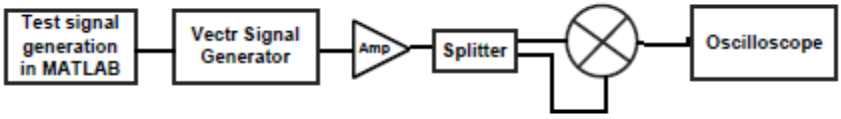


Fig. 13: Hardware measurement block diagram

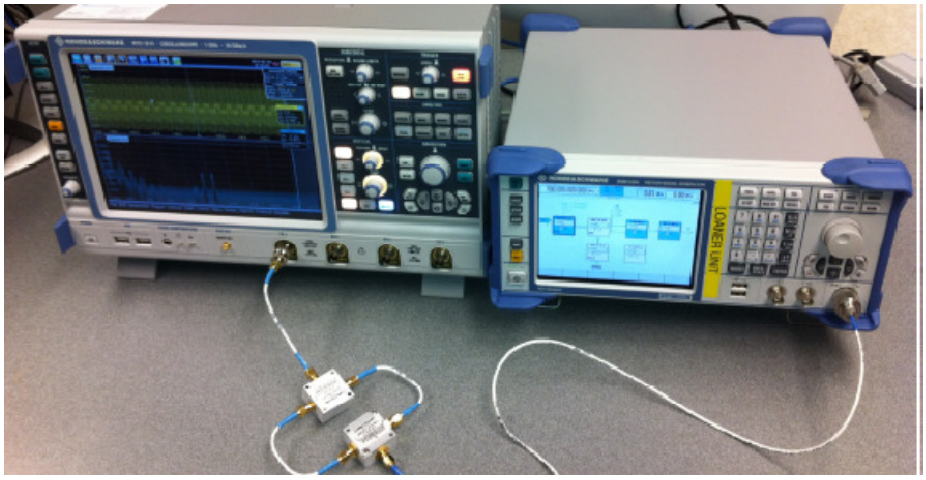

Fig. 14: Hardware measurement setup

Different cases of impairments are generated and tested to evaluate the accuracy of the technique. Fig. 15 shows a sample of the time domain captures at the output of the BiST circuitry and the spectrum of this signal is presented in Fig. 16. As expected, the frequency domain response includes ω1, ω2 and the intermodulation products. The desired signal components are at 1MHz, 4MHz, 5MHz, 8MHz,

9MHz and 10MHz. We observe from Fig. 16, that there are additional harmonics and intermodulation products that have been generated due to the limited quality LO signal. By carefully adjusting our signal frequencies and using FFT, we can prevent these undesired components from corrupting the desired information. Such isolation would not be possible if we were using time domain information. The advantage of the proposed method is that even if there are unmodeled components in the signal, we can still preserve the necessary information.

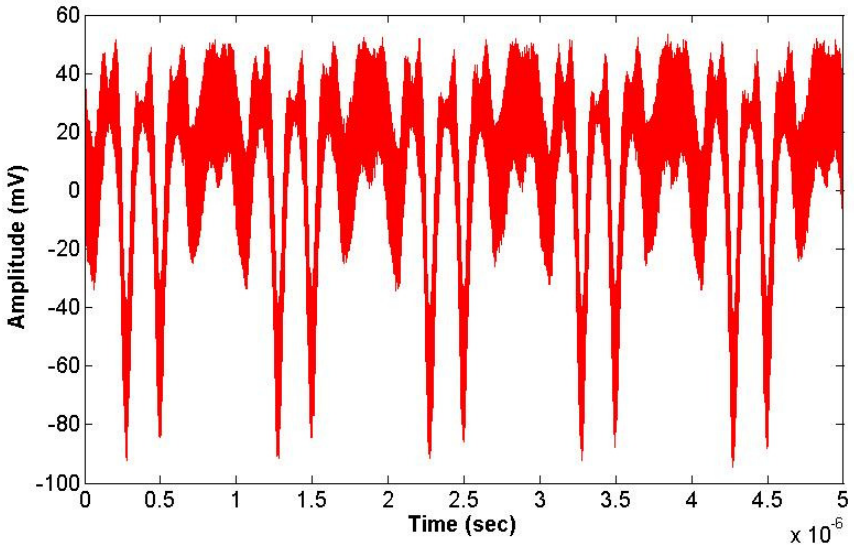


Fig. 15: Hardware measurement time domain output

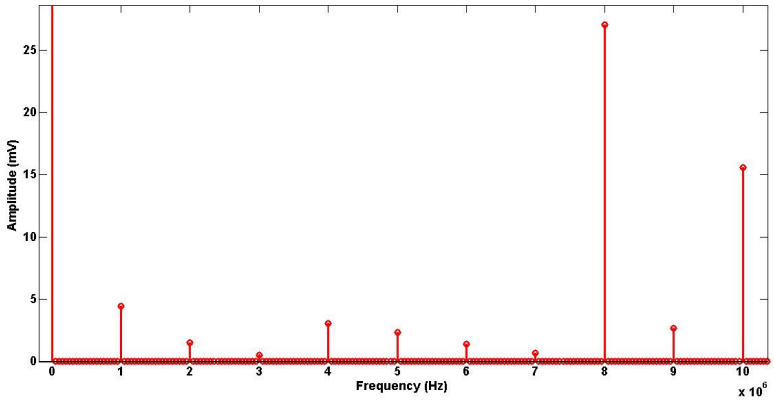


Fig. 16: Hardware measurement spectrum output

| Cases | Parameter | Actual | Computed | Error |
|---|---|---|---|---|
| Case -1 | $g_{tx}$ | -5% | -5.1% | 0.1% |
| | $\varphi_{tx}$ | -1° | -1.1° | 0.1° |
| | $DC_{Itx}$ | 10mV | 12.6mV | 2.6mV |
| | $DC_{Qtx}$ | 10mV | 10.6mV | 0.6mV |
| Case - 2 | $g_{tx}$ | 15% | 16% | 1% |
| | $\varphi_{tx}$ | 4° | 4.37° | 0.37° |
| | $DC_{Itx}$ | 20mV | 23.2mV | 3.2mV |
| | $DC_{Qtx}$ | 30mV | 19.7mV | 10.3mV |
| Case -3 | $g_{tx}$ | 20% | 21% | 1% |
| | $\varphi_{tx}$ | 5° | 5.47° | 0.47° |
| | $DC_{Itx}$ | 10mV | 10.5mV | 0.5mV |
| | $DC_{Qtx}$ | 20mV | 9.1mV | 10.9mV |

Table III: Hardware results of I/Q impairments extraction

Table III shows 3 cases of the measurement results. Gain mismatch can be measured with 1% error whereas phase mismatch is measured with up to 0.5° error. DC offset in I and Q arms is measured with up to 10mV error. As expected, measurements display slightly higher error

due to noise in the system, equipment limitations, and potential unmodeled behavioral deviations. However, the errors are well within acceptable range.

Nonlinear mode hardware measurements:.

IIP3 of the amplifier under study is first measured using the conventional method for comparison. The test setup to measure the IIP3 is shown in fig. 17.

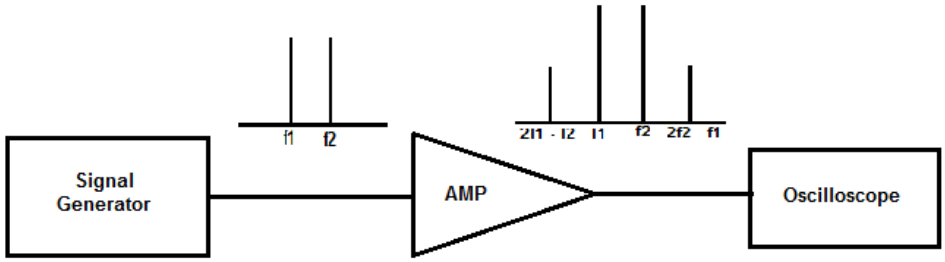


Fig. 17: Test setup to measure IIP3

A closely spaced two tone signal is fed as input to the amplifier and IIP3 is calculated using the eqn. 16, in which all parameters are expressed in dB.

$$IIP3 = \frac{(P_{fundamental} - P_{intermod})}{2} + P_{input} \qquad (16)$$

From the measurements, IIP3 of amplifier was calculated as 5.82dB which was in close accordance with the value in the data sheet which was 5.8dB.

IIP3 of the system was measured using the proposed method on hardware. There are two steps to extract IIP3 using the analytical BiST approach. First, excite the system shown in fig in the linear

mode (lower input power). Extract $\left(\frac{G}{K}\right)$ using eqn.5. Then excite the system in the non linear mode (higher input power). Extract $\left(\frac{G3}{K}\right)$ using eqn. 12. Substitute both $\left(\frac{G}{K}\right)$ and $\left(\frac{G3}{K}\right)$ in eqn. 14 to obtain IIP3 of the system. With same inputs of 5Mhz on I channel and 4Mhz on Q channel. The required information to extract $\left(\frac{G3}{K}\right)$ is available at 30 MHz. It should be ensured that if a low pass filter is present then the cutoff frequency of the filter is above 6ω1, that is 30Mhz in this case.

| Cases | Actual IIP3 (dB) | Extracted IIP3 (dB) | Error (dB) |
|---|---|---|---|
| Case 1 – ($g_{tx}$ = 10%, $\varphi_{tx}$ = 1°, $DC_{Itx}$ = 10mV, $DC_{Qtx}$ = 20mV) | 5.8 | 5.67 | -0.12 |
| Case 2 – ($g_{tx}$ = 15%, $\varphi_{tx}$ = 4°, $DC_{Itx}$ = 20mV, $DC_{Qtx}$ = 30mV) | 5.8 | 6.13 | 0.33 |
| Case 3 – ($g_{tx}$ = 20%, $\varphi_{tx}$ = 5°, $DC_{Itx}$ = 10mV, $DC_{Qtx}$ = 20mV) | 5.8 | 5.96 | 0.16 |

Table 4: Hardware results of IIP3 extraction

Two important specifications have to be ensured for the nonlinear measurements:

1. For the measurements on hardware, it should be ensured that the dynamic range of the oscilloscope used to measure should be higher than the dynamic range of the output at the BiST circuitry.
2. As seen in eqn. 11, there are many frequency terms at the baseband. So proper coherent sampling of the signal has to be ensured, in the absence of which the signal from the adjacent frequency will affect the measurement.

Three cases of impairments were setup on the I/Q transmitter along with amplifier and IIP3 values were extracted. Table IV shows the actual and extracted values of IIP3 of the system along with the error. It shows the change in impairments have no affect on the measurement of IIP3 as it depends only on $\left(\frac{G}{K}\right)$ and $\left(\frac{G3}{K}\right)$ measured. It can be seen that method provides excellent results of the IIP3 extraction on hardware.

Chapter 6

# ADVANTAGES AND LIMITATIONS

## 6.1: ADVANTAGES

- Determination of all I/Q imbalances (gain and phase mismatch, DC offsets, time skews) with a single set up.
- Analytical computation as opposed to using non-linear solvers or any sort of search criterion
- Very efficient measurement with almost no computational overhead
- Using frequency domain information to suppress the effects of undesired and/or unmodeled circuit effects.
- High accuracy despite using only low-frequency information.
- The method can also be implemented with external components on existing devices to reduce test cost.

## 6.2: LIMITATIONS

- Two steps are required to extract nonlinearity.
- Since the all parameters are extracted analytically, error in one parameter will result in error in the subsequent parameter extraction.

- Coherent sampling of the output signal is a necessity for the validity of the method. Hence, number of samples required can vary based on the frequency of baseband signal.

# Chapter 7

# CONCLUSION

A BiST solution for transmitter IQ imbalances and nonlinearities measurement was proposed. Testing high frequency devices requires using expensive RF measurement equipment. We design a BiST circuitry to convert this signal to a simpler form. For low-frequency conversion, we use a self mixing envelope detector. The proposed BiST circuitry along with designed test signal enables us to derive the transmitter impairment measurement with low computational complexity. The frequency domain information of the envelope signal is used to mathematically solve for the I/Q imbalances and nonlinearities. Simulations along with hardware measurements confirm the accuracy of the technique. As simple mathematical expressions are followed to solve for the impairments, the method is very straightforward and simple. The hardware results obtained are also very encouraging. Hence, paving the way for on-chip circuit characterization and calibration.

# REFERENCES


[1] "Ericcson Traffic and Market report", www.ericcson.com

[2] S. Bhattacharya, A. Chatterjee, "Use of Embedded Sensors for Built-in-Test RF Circuits" in *International Test Conference 2004.*

[3] S. Bhattacharya, A. Chatterjee, "A Built-in Loopback Test Methodology for RF Transceiver Circuits using Embedded Sensor Circuits" in *13th Asian Test Symposium, November 2004, pp. 68–73.*

[4] H. Hsieh, L. Lu, "Integrated CMOS Power Sensors for RF BIST Applications" in *24th IEEE VLSI Test Symposium, May 2006.*

[5] Y. Huang, H. Hsieh, L. Lu, "A Low-Noise Amplifier with Integrated Current and Power Sensors for RF BIST Applications," *VLSI Test Symposium, IEEE, 2007*

[6] M.J. Barragan, R Firoelli, D Vazquez, A Rueda, J.L. Huertas, "Low-Cost Signature Test of RF Blocks Based on Envelope Response Analysis" in IEEE *European Test Symposium, (ETS), May 2010, pp. 55–60.*

[7] K. Yanagisawa, N. Matsuno, T. Maeda, S. Tanaka, "A New DC-Offset and I/Q-Mismatch Compensation Technique for a CMOS Direct-Conversion WLAN Transmitter" in *IEEE Microwave Symposium, June 2007.*

[8] D. Han, A. Chatterjee, "Robust Built-in Test of RF ICs Using Envelope Detectors" in *4th Asian Test Symposium, December 2005.*

[9] M. Valkama, M. Renfors, and V. Koivunen, "Advanced methods for I/Q imbalance compensation in communication receivers," *IEEE Transactions on Signal Processing, pp. 2335–2344, Oct 2001.*

[10] E. Erdogan and S. Ozev, "Detailed characterization of transceiver parameters through loop-back-based BIST," *IEEE Transactions on Very Large Scale Integration (VLSI) Systems, pp. 901–911, 2010.*

[11] A. Banerjee, V. Natarajan, S. Sen, A. Chatterjee, G. Srinivasan, and S. Bhattacharya, "Optimized Multitone Test Stimulus Driven Diagnosis of RF Transceivers Using Model Parameter Estimation," in *International Conference on VLSI Design, January 2011, pp. 274 –279.*

[12] F. Poehl, F. Demmerle, J. Alt, H. Obermeir, "Production Test Challenges for Highly Integrated Mobile Phone SOCs- A Case Study" in *15th IEEE European Test Symposium, May 2010.*

[13] L. Dermentzoglou, A. Arapoyanni, and Y. Tsiatouhas, "A Built-In-Test Circuit for RF Differential Low Noise Amplifiers," *IEEE Transactions on Circuits and Systems I: Regular Papers, pp. 1549–1558, July 2010.*

[14] A. Gopalan, T. Das, C. Washburn, and P. R. Mukund, "An Ultra-Fast, On-Chip BiST for RF Low Noise Amplifiers." in *VLSI Design, 2005, pp. 485–490.*

[15] S. Sermet Akbay and A. Chatterjee, "Built-in test of RF components using mapped feature extraction sensors," in *23rd IEEE VLSI Test Symposium, May 2005, pp. 243–248.*

[16] A. Valdes-Garcia, W. Khalil, B. Bakkaloglu, J. Silva-Martinez, and E. Sanchez-Sinencio, "Built-in Self Test of RF Transceiver SoCs: from Signal Chain to RF Synthesizers," in *IEEE Radio Frequency Integrated Circuits (RFIC) Symposium, June 2007, pp. 335–338.*

[17] D. Lupea, U. Pursche, and H.-J. Jentschel, "RF-BIST: loopback spectral signature analysis," in *Design, Automation and Test in Europe Conference and Exhibition, 2003, pp. 478–483.*

[18] J.-Y. Ryu, B. Kim, and I. Sylla, "A new low-cost RF built-in self-test measurement for system-on-chip transceivers," *IEEE Transactions on Instrumentation and Measurement, pp. 381–388, April 2006.*

[19] M. Barragan, R. Fiorelli, D. Vazquez, A. Rueda, and J. Huertas, "On-chip characterization of RF systems based on envelope response analysis," *Electronics Letters, pp. 36–38, July 2010.*

[20] D. Han, S. Bhattacharya, and A. Chatterjee, "Low-cost parametric test and diagnosis of RF systems using multi-tone response envelope detection," *Computers Digital Techniques, pp. 170–179, May 2007.*

[21] J. de Witt and G.-J. van Rooyen, "A blind I=Q imbalance compensation technique for direct-conversion digital radio transceivers," *IEEE Transactions on Vehicular Technology, pp. 2077–2082, May 2009.*

[22] A. Tarighat, R. Bagheri, and A. Sayed, "Compensation schemes and performance analysis of IQ imbalances in OFDM receivers," *IEEE Transactions on Signal Processing, pp. 3257–3268, Aug. 2005.*

[23] E. S. Erdogan, Sule Ozev, "Single-Measurement Diagnostic Test Method for Parametric Faults of I/Q Modulating RF Transceivers," *in Proc. 26th VLSI Test Symp., May 2008*.

[24] B. Razavi, "RF Microelectronics," *Prentice Hall, NJ 1998*.

[25] Thomas H. Lee, "The Design of CMOS Radio-Frequency Integrated Circuits," *Cambridge University Press, second edition.*

[26] G. Roberts, F. Taenzler, M. Burns, "An introduction Mixed-signal IC Test and Measurement", *Oxford University press, second edition.*



46